

Microstructure and strain relief of Ge films grown layer by layer on Si(001)

F. K. LeGoues, M. Copel, and R. M. Tromp

IBM Research Division, Thomas J. Watson Research Center, Yorktown Heights, New York 10598

(Received 8 June 1990)

We have studied the microstructure of Ge films grown layer by layer on Si(001) surfaces. The growth mode was changed from a Stranski-Krastanov mode (layer by layer for 3 monolayers, followed by islanding) to a layer-by-layer growth mode by passivation of the surface with 1 monolayer of arsenic. This change in growth morphology results in drastic changes in the mechanism of strain relief. Unlike films grown on bare Si, these films remain pseudomorphically strained up to a thickness of about 10 monolayers. At a film thickness of 12 monolayers, we observe the catastrophic formation of strain-induced defects. These consist of several {111} planes tilted perpendicular to the substrate. The defects are V-shaped and, consequently, relieve the misfit progressively as the film grows. At a film thickness of 50 monolayers, we observe that the V-shaped defects serve as nucleation sites for dislocations that climb down into the Si substrate. These dislocations then glide through the film to relieve the misfit in previously undefected areas. Thus, the misfit is relieved partly by V-shaped defects located in the Ge layer and partly by edge dislocations located in the Si substrate. For thick films, we observe that most of the V-shaped defects have been covered by Ge oriented epitaxially with the substrate, but they have also generated twins and stacking faults that extend throughout the whole film. This work has fundamental implications for the understanding of strain relief during "normal" growth. Indeed, it demonstrates that the so-called critical thickness has to take into account the formation energy of the strain-relieving defects (in general, dislocations), and not only the energy to move the defects, as has generally been done up to now.

I. INTRODUCTION

Strain and strain-relief mechanisms play a considerable role in determining the microstructure and electronic properties of thin films. For example, strain can change the band gap in thin Si/Si-Ge (or Si/Ge) multilayers. To obtain technologically useful materials, it is important in this case to completely inhibit the formation of defects. This can be accomplished by working well below the "critical thickness" at which it becomes energetically more favorable to generate strain-relief defects (generally dislocations) rather than strain the film as a whole. This limits the range of thickness and composition, and thus the electronic properties, that can be achieved. On the other hand, relaxed films are also important, providing new substrates for complicated structures. For example, a completely relieved Ge layer on Si could be used to grow undefected GaAs layers on Si, since Ge and GaAs are lattice-parameter-matched. The problem here is to obtain a relaxed layer where the strain-relief defects do not extend through the film, but are buried, so that the top surface remains perfect. In general, this is very hard to control as both pure edge dislocations and threading dislocations are formed during growth. Thus, understanding and controlling strain-induced defects and their mechanism of formation are critical to further use and development of thin epitaxial films for technology.

Ge normally grows in the Stranski-Krastanov mode on Si(001), i.e., it grows layer by layer for 3 monolayers, and forms islands thereafter. This is explained by the fact that, even though Ge has a lower surface free energy than Si (thus the initial layer-by-layer growth), the strain be-

comes too high very fast, rendering island growth more favorable. When islands are formed, it is easy to visualize how dislocations are introduced at the interface: dislocations can nucleate at the edge of islands and then glide underneath the island. When a complete layer is finally achieved, the network of dislocations is already established. The problem in this case is that, when the islands meet, they tend to generate threading dislocations, and sometimes other defects such as twins.

Recently, Copel *et al.*^{1,2} and LeGoues *et al.*³ have shown that Ge growth on Si(001) can be drastically altered by using a monolayer of arsenic as a growth controlling "surfactant." The growth mode changes from Stranski-Krastanov to layer by layer, which has a considerable effect on the film morphology and microstructure. Indeed, it was shown that, in this case, misfit dislocation formation is completely inhibited.³ Instead, a strain-induced defect was observed. These findings demonstrate the importance of growth mode on final microstructure.

In this paper we investigate the morphology, microstructure, and strain-relief mechanisms for thin Ge films grown with an As surfactant, in a range of thicknesses from 8 to 65 monolayers. The thinnest films (8 monolayers) are completely strained and pseudomorphic, i.e., no defects and/or islands are formed. At a thickness of 12 monolayers, previously described³ strain-induced defects have formed throughout the film. These consist of several {111} planes tilted perpendicular to the direction of maximum strain, and forming a V-shaped defect. These defects have the remarkable characteristic of relieving the misfit progressively, so that, in principle, they could relieve the film as it grows, without having to intro-

duce any other defect. At film thicknesses of about 50 monolayers, we nonetheless observe that, instead of growing, the defects act as "injection" sites for edge dislocations that climb down into the Si substrate and then glide through the rest of the sample. Thus, the strain relief is now shared by the original defects in the Ge layer, and dislocations located in the silicon substrate. Finally, at the highest thickness investigated, we find that some of the defects are overgrown by undefected Ge, leaving a perfect Ge layer on top. However, the majority of the defects generate extended defects growing all the way through the Ge films. These are mainly stacking faults which probably play the dual role of minimizing interfacial energy between the defects and the rest of the film and of relieving any remaining strain.

We discuss the mechanisms of formation of the observed defects, the strain-relief mechanisms operating in this system, and the implications on formation of dislocations during "normal" growth. Possible uses of this growth technique for growing perfect, relaxed Ge films are considered.

II. EXPERIMENTAL TECHNIQUE

The growth technique used in this study was described in detail in Refs. 1 and 2. Briefly, Si samples were cleaned by mild sputtering followed by a short flash at 1050°C. Ge was deposited in UHV at 500°C at rates of about 0.3 monolayer/min. The Si surface was passivated

by 1 monolayer of As prior to Ge growth, and an overpressure of As was supplied during growth. For the thinner samples, a Si cap was deposited on the Ge film in order to avoid oxidation and loss of Ge. Samples were prepared for both planar view and cross-sectional transmission electron microscopy observation by mechanical thinning to about 50 μm , and then ion milling to electron transparency. Samples were observed on a Philips 430 microscope operating at 300 kV and on a JEOL 4000 microscope operating at 400 kV.

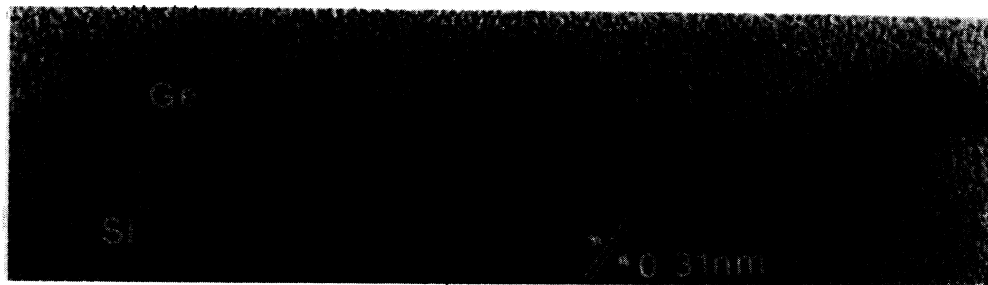
III. RESULTS

A. Growth without arsenic

Figure 1(a) shows a cross-sectional micrograph of 8 monolayers of Ge [1 monolayer (ML) = 6.78×10^{14} atoms/cm²] deposited on a clean Si(001) substrate. The Ge film has agglomerated in epitaxial, pseudomorphic islands. After further growth [Fig. 1(b)], the islands have grown in size, and are no longer pseudomorphic, as the appearance of misfit dislocations at the Si/Ge interface (see arrows) clearly indicates.

B. Growth with arsenic

In contrast, Fig. 2(a) shows a Si/8 ML Ge/Si(001) sample grown with a monolayer of As present on the surface.



(a)



(b)

FIG. 1. Cross-sectional views of samples grown without surfactant. (a) 8 monolayers. Note that the islands are still pseudomorphic. (b) 15 monolayers. Arrows indicate the presence of dislocations at the interface between the island and the substrate.

Although growth rate and temperature were the same as in Fig. 1(a), islands are now conspicuously absent. The Ge film is epitaxial, pseudomorphic, and uniform in thickness.

1. V-shaped defects

Figure 2(b) shows the microstructure of a 12 monolayer film of Ge. First, it is clear that the Ge layer is still continuous, and that layer-by-layer growth has been maintained. Secondly, we now observe the appearance of strain-induced defects [indicated by an arrow in Fig.

2(b)]. Figure 3 shows a planar view of this sample and, for comparison, of a similar sample grown without surfactant. When no surfactant is used, small islands of Ge are observed, which have the lattice parameter of bulk Ge. This can be concluded both from the observation of Moire fringes on the image and from the splitting of the diffraction spots [see also Fig. 1(b)]. The sample grown with As shows a uniform background (no islanding), and numerous linear defects aligned along the $\langle 110 \rangle$ directions. These defects give rise to extra diffraction spots corresponding to a lattice spacing of 0.31 nm, which is the $\{111\}$ spacing for Si or Ge [see the diffraction pattern

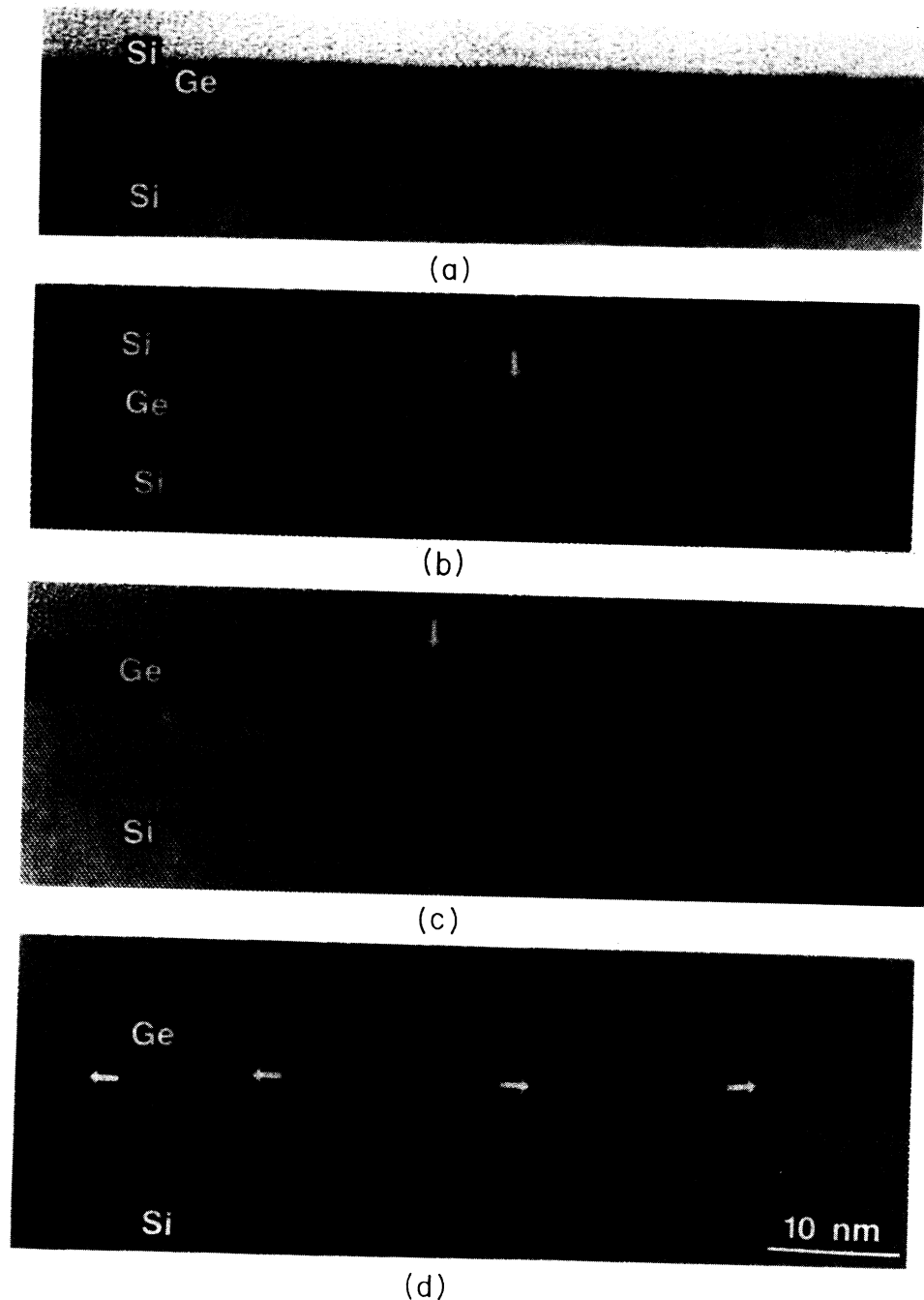


FIG. 2. Cross-sectional views of the samples grown with an arsenic surfactant. (a) 8 monolayers; (b) 12 monolayers; (c) 50 monolayers; (d) 65 monolayers.

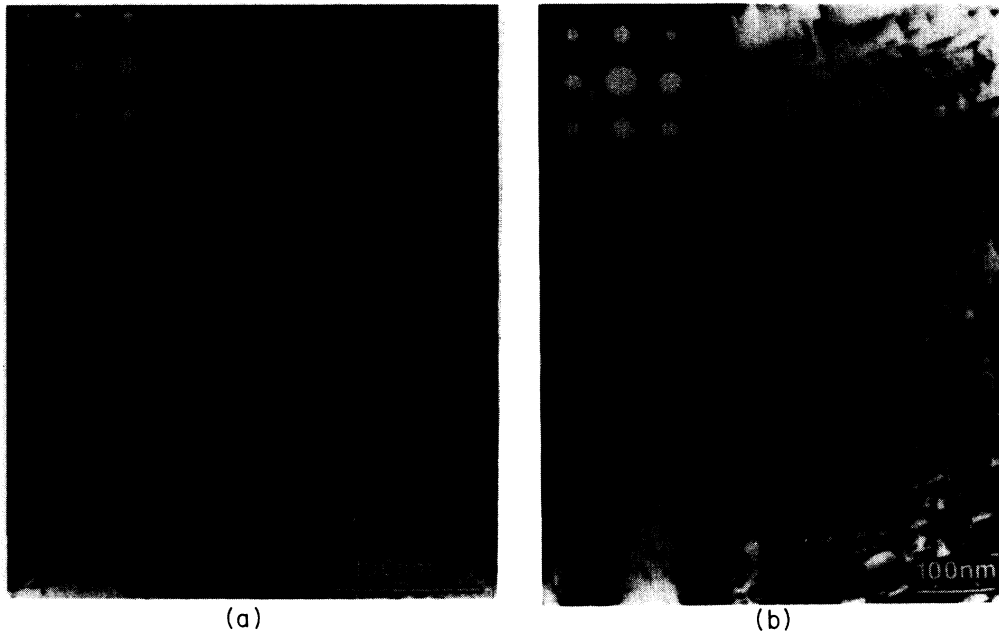


FIG. 3. Planar view of 12 monolayers grown on (a) bare Si and (b) arsenic passivated Si. The arrow on the diffraction pattern on (a) indicates the splitting of the spots showing that Ge has the lattice parameter of bulk Ge. The arrows on (b) show the extra spots associated with the V-shaped defects.

in Fig. 3(b)]. This indicates that the thin defects correspond to platelets in which the $\{111\}$ lattice planes are oriented perpendicular to the substrate. Another important observation is the lack of Moire fringes. Figure 4 shows a high-resolution cross-sectional view of the defect as well as an atomic model. The corresponding simulated⁴ image shows good agreement with the experimental image. The defect can be described as several (three to five) $\{111\}$ planes tilted perpendicular to the substrate. The defect forms a V, where each branch of the V lies along a $\langle 112 \rangle$ direction. Thus the boundary between the defect and the rest of the Ge film can be described as a $\Sigma 9$ boundary,^{5,6} i.e., a symmetric tilt boundary with a tilt an-

gle of 38.94° and a $\{110\}$ tilt plane. We note that, since each $\Sigma 9$ boundary defines a microcrystal related to the other by a twin (located at the center of the defect), and the twin is by definition symmetric, the actual tilt angle of the boundaries has to be 35.26° (the angle between the $[001]$ and the $\langle 112 \rangle$ directions in a cubic crystal). Thus a disclination of 3.68° exists at each boundary which has to be accommodated by strain.

2. Misfit dislocations

The second stage of strain relaxation is defined by the appearance of edge dislocations in the Si substrate, and is

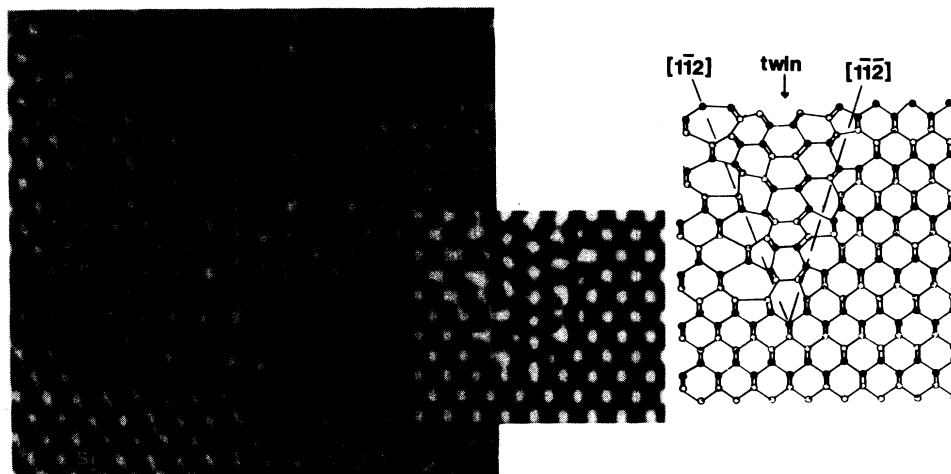


FIG. 4. Cross-sectional view of one defect in the 12-ML film, atomic model, and corresponding image simulation (the parameters for the simulations are described in Ref. 11).

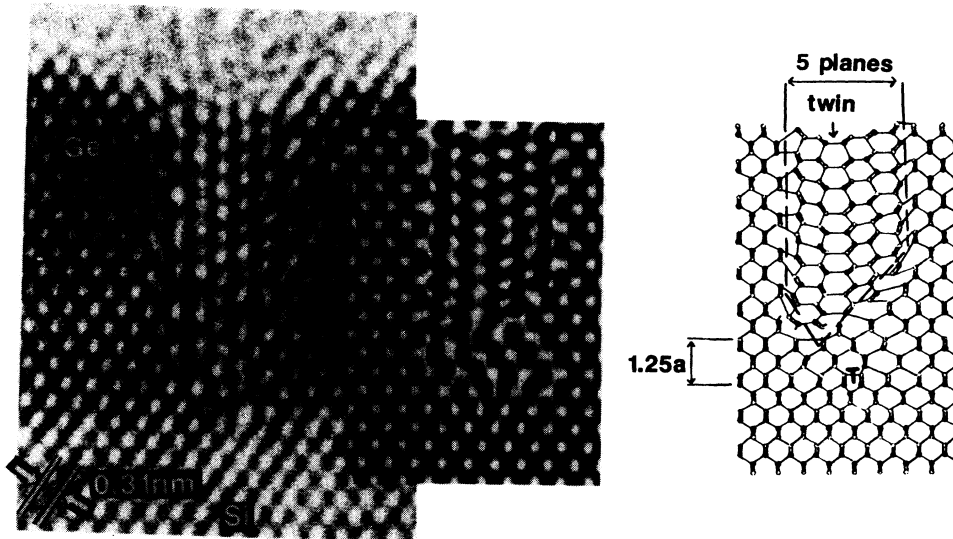


FIG. 5. Cross-sectional view, atomic model, and simulation of one defect in the 50-ML film.

exemplified in Figs. 2(c), 5, and 6. Figure 2(c) shows a 50 monolayer Ge film. Defects are very similar to that described in Fig. 4, i.e., they correspond to several $\{111\}$ planes tilted perpendicular to the substrate. A twin is present at the center of the defect forming two microcrystals. Close inspection of this defect indicates several differences with the ones observed in thinner films. One example is shown at high magnification in Fig. 5. First, the defect is now no longer V shaped: instead, its boundaries now lie along the $[001]$ direction, perpendicular to the substrate (although, for the sake of simplicity, we will keep referring to these as V-shaped defects). Secondly, a pure edge dislocation has now appeared inside the Si substrate itself. This can be made more obvious by drawing a Burger circuit, confined in the Si, at the tip of the defect. Several examples are shown in Fig. 6, and Fig. 5 shows an atomic model of one of the defects, where the location of the dislocation has been indicated. In Fig. 6(b) we show one defect that has been overgrown by undefected Ge, so that a Burgers circuit can be drawn around the V-shaped defect itself, showing a Burgers vector equal to $a/\sqrt{2}$, equivalent to a pure edge dislocation in Si. The total Burgers vector for the V-shaped defect and its associated dislocation is $a\sqrt{2}$, or two pure edge dislocations. All of the V-shaped defects observed at this thickness were associated with an edge dislocation located at some depth in the Si substrate. Figure 7 shows a planar view of the sample. When viewed exactly perpendicular to the substrate, along the $[001]$ direction, the sample only shows a well-defined set of Moire fringes, indicating a difference in lattice parameter between some part of the film and the substrate (this can also be seen from the splitting of the diffraction spots). By tilting the sample off the exact $[001]$ zone axis by a few degrees, we can greatly reduce the contrast of the Moire fringes, so that the square, if somewhat irregular and wavy, network of dislocations is now easily observed [Fig. 7(b)]. Dark field micrographs obtained from the reflections due to the

V-shaped defects are shown in Fig. 7(c) and 7(d). Each defect is associated with a dislocation that then extends to other parts of the samples. Most dislocations meander from one defect to another, thus accounting for the waviness of the network.

3. Other defects

Figure 2(d) shows a thick Ge film (65 monolayers). At this relatively low magnification, several defects are visible. Some seem similar to the ones described above, while some seem to be only microtwins or stacking faults. All of the defects are again accompanied by edge dislocations located at some depth in the Si substrate. Thick layers were grown in the hope that the V-shaped defects would eventually be overgrown by an undefected and relaxed top Ge layer. Figure 8 shows that, in a few instances, this indeed happens: here we have a V-shaped defect, similar to the ones described earlier, which has been overgrown by perfect Ge. The Burgers circuit shows that the defect, with its associated dislocation, is equivalent to two pure edge dislocations, so that the strain between the Ge layer and the Si substrate could indeed be relieved by a network of V-shaped defect-associated dislocation with an average distance of about 190 Å. Unfortunately, this type of overgrowth does not seem to be the norm, as seen in Fig. 9, which shows several typical defects observed in the thick film. Figure 9(a) shows an example where, in order to achieve a low-energy boundary between the V-shaped defect and the overlying Ge films, a secondary twin has appeared on top of the defect. In this case, the boundary between the V-shaped defect and the overlayer is a simple twin, which should add very little energy to the film. On the other side of the defect a stacking fault also helps to match the defect with the overlayer. Figure 9(b) shows an instance where the V-shaped defect has kept growing, forming nonsymmetric grain boundaries along the $[001]$ direction between the defect and the rest

of the film. Again, toward the top of the film, where undefected Ge may be trying to overgrow the defect, a stacking fault has appeared. Figure 9(c) shows an example where the V-shaped defect has been completely overgrown by Ge with the same orientation as the substrate, but several stacking faults have also been generated at the top of the defect. Finally, Fig. 9(d) shows two stacking faults forming a V, which were probably generated by a

defect, but have extended further in the undefected film. Note that they are also associated with a dislocation in the Si substrate.

IV. DISCUSSION

In most theoretical predictions of critical thickness, it is implied that the formation energy of dislocations is negligible. Indeed, in the generally used theory^{7,8} governing strain relaxation by dislocations, the so-called "critical thickness," as defined by Matthews and Blakeslee,^{7,8} is a simple balance between the energy necessary to strain the layer and the energy expended by moving *existing* dislocations. In this definition (also discussed by Van der Merwe⁹), no discussion is made of the need to *nucleate* dislocations. It is assumed that the dislocations will be provided by the substrate. While this assumption was valid when Matthews and Blakeslee wrote their original paper (and may still be for GaAs substrates), today's Si substrates have negligible numbers of dislocations to provide to the interface, so that all the dislocations have to be nucleated somewhere else. Consequently, Matthews and Blakeslee's theory consistently gives significantly lower critical thicknesses than experimentally observed in the SiGe case. This demonstrates that the nucleation energy plays an important role in determining critical thickness. It is indeed somewhat remarkable that none of the theoretical treatments take the morphology of the film into account. Clearly, if islands are formed, the nucleation energy of a dislocation at the edge of an island is nearly negligible. Indeed, it is generally assumed that this is the driving force for island formation in the Ge/Si system. This somehow assumes that the Ge films "know" that, once islands have formed, it will be easier to introduce dislocations, which is unlikely. It also would require that, as soon as islands are observed, so are dislocations. Recently Eaglesham and Cerullo¹⁰ shows that very large islands can form without introducing dislocations. Also, in the present work, Fig. 1(a) shows completely pseudomorphic islands. Thus, the driving force to island formation cannot be the introduction of dislocations. Kirchner and Chilshom¹¹ demonstrated that, past a certain thickness determined by the misfit, strain would render a thin film unstable to small thickness fluctuations, thus the eventual formation of islands. Once islands have formed though, it is easy to introduce dislocations that can then glide underneath the island [see Fig. 1(b)]. Thus, once a continuous layer is eventually formed, the network of dislocation is already present.

When arsenic is used as a surfactant, the morphology of the film is drastically altered. Indeed at a thickness of 8 monolayer, we observe uniform, undefected Ge films. This is already significantly over the thickness at which dislocations were previously observed³ in the same growth conditions, but without a surfactant. In other words, two microstructural changes have occurred. First, no islands have formed. Secondly, no dislocations have formed, showing the correlation between island formation (or ease of dislocation nucleation) and critical thickness. Matthews and Blakeslee suggested that, when not enough substrate dislocations are available, new dislocations can form by "looping" from the surface. In

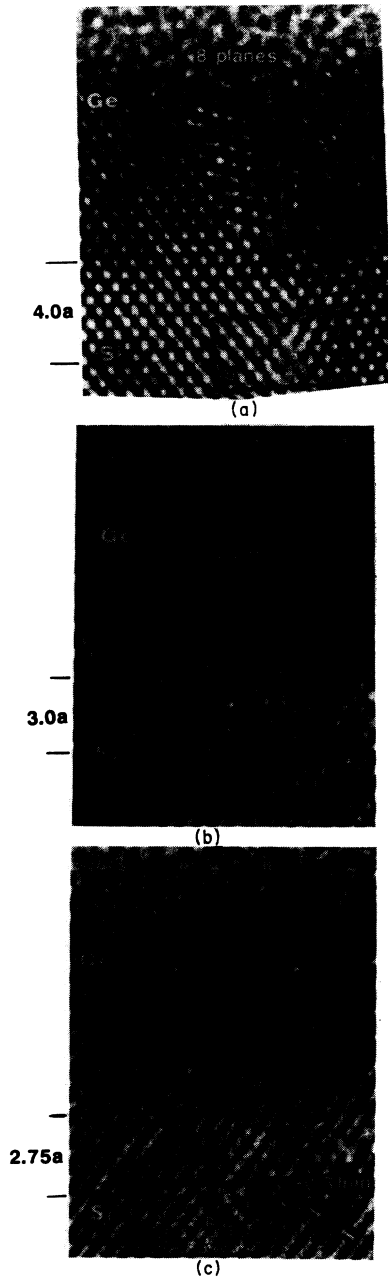


FIG. 6. Other defects found in the 50-ML film. Burgers circuit have been drawn, entirely contained in the Si substrate, that locate the edge dislocations. In (b), a Burgers circuit has also been drawn around the defect to demonstrate that it is equivalent to a dislocation.

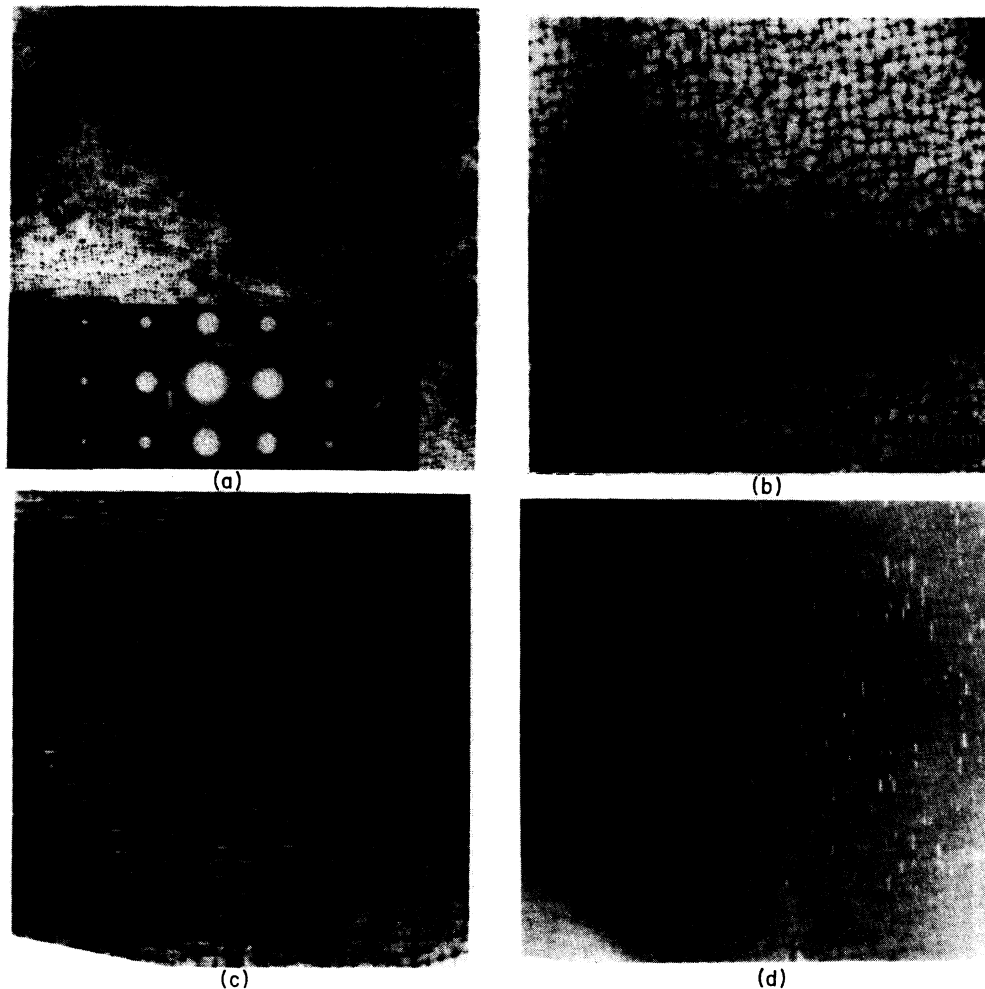


FIG. 7. Planar view of the 50-ML sample. (a) The zone axis is exactly [001], or perpendicular to the substrate. Arrows in the diffraction pattern indicate the extra reflections due to the defects. (b) Same area. The sample has been tilted off the exact zone axis by a few degrees in order to lower the contrast of the Moire fringes and image the dislocation network. (c) and (d) Dark field micrographs obtained using the reflections marked by arrows in (a).

their calculations of the critical thickness, they did not take into account any nucleation energy for dislocation loops, thus assuming in effect that this energy is negligible. In our case looping is not observed and dislocation formation is inhibited.

Let us reexamine the notion of critical thickness. By definition, the critical thickness is the thickness at which some strain-induced defect will start relieving the misfit. In some instances, this may correspond to the thickness at which dislocations can move, provided that dislocation nucleation is easy. In the present case, the critical thickness is limited by the nucleation of the V-shaped defects. This indicates that the formation energy of a V-shaped defect is lower than the formation energy for dislocation loops.

In the absence of dislocations, a very effective way to relieve strain is to position {111} planes perpendicular to the substrate, i.e., to position the close-packed planes perpendicularly to the direction of maximum strain. This

occurs between 8 and 12 monolayers. From the observation that the defects are small, randomly distributed, and disconnected from each other, we infer that the defect formation occurs catastrophically. At this stage of growth, the defect boundaries are completely coherent with the rest of the film, and its energy cost should be similar to that of an equivalent dislocation.³

Since the defect is V-shaped, it grows wider as the Ge films grows thicker, thus relieving more and more of the misfit. This explains the observed lack of Moire fringes [Fig. 3(b)], since the lattice parameter changes continually throughout the Ge film. After initial formation of defects [Figs. 2(b), 3(b), and 4], about one-third of the strain has been relieved. Eventually, with an average distance between defects of about 200 Å, the strain could be completely relieved, without generating any new defect, at a film thickness of about 50 Å, when the width of the defects have reached an average of 12 [111] planes.³

Surprisingly, Figs. 5, 6, and 7 show that there is a dis-

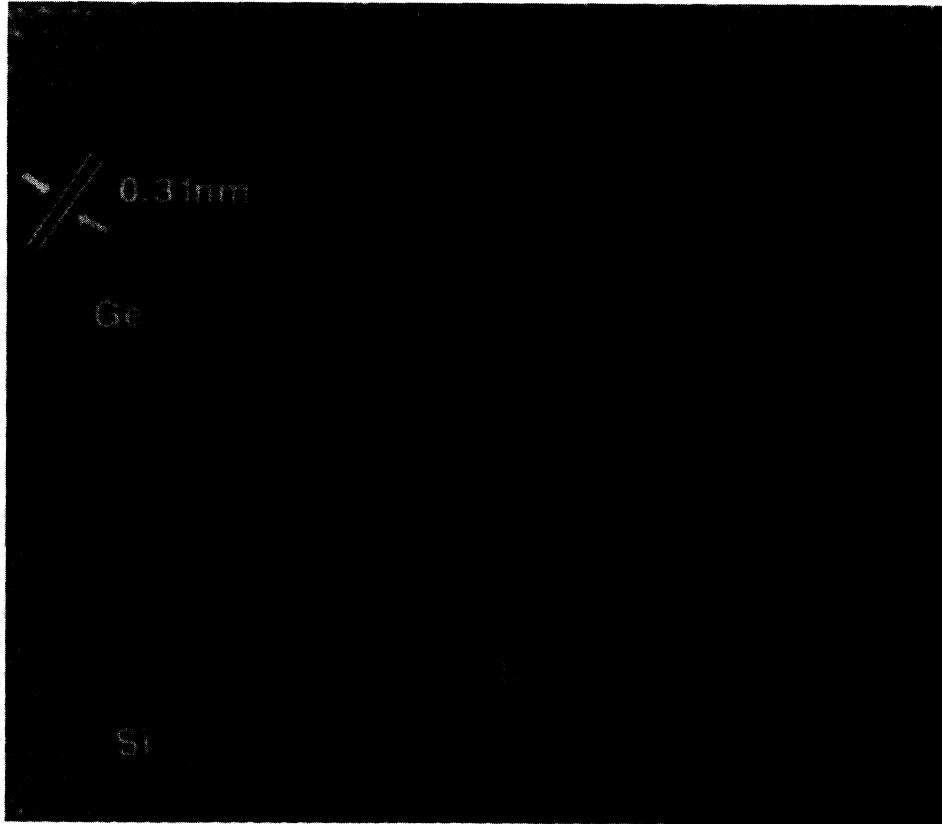


FIG. 8. One defect in the 65-ML film that has been completely covered by undefected Ge. A Burgers circuit has been drawn around the defect, and its associated dislocation, which show that, together, they are equivalent to two pure edge dislocations.

tinct change of microstructure before the film is fully relaxed. At about half the thickness at which we expect complete accommodation of the misfit, the boundaries of the defect become perpendicular to the Si substrate. In order to keep relieving the misfit progressively, the defect would have to keep the same configuration, i.e., several $\{111\}$ planes bounded to the undefected film by $\Sigma 9$ boundaries and forming a twin in the center of the defect. This configuration generates a disclination of 3.68° at each $\Sigma 9$ boundary, or a total disclination of 7.36° at the center twin (see Ref. 3). When the defect is small, as is the case for the thin film shown in Figs. 3 and 4, this disclination can simply be accommodated by a slight stretching of the atomic bonds in the defect, but eventually, such a configuration would become unstable. Thus, the extra strain energy within the defect prevents its propagation as a widening V before all the misfit has been accommodated. We have pointed out earlier that the defects form because of the lack of energetically favorable nucleation sites for dislocations. However, the boundaries of the defect is composed of several five-bounded ring and seven-bounded ring units (see Figs. 4 and 6), which are identical to the core of a dislocation in Si. Thus, a dislocation can climb down from the top of the

defect, along the grain boundary. Thus, only diffusion away from the defect will be necessary to inject a dislocation into the substrate. We note that diffusion to and from the surface of the film is expected to be easy, since the walls of the V-shaped defect are in fact grain boundaries. We can speculate as to the exact mechanism by which the dislocations are introduced: the intersection of the defect with the surface may provide an easy nucleation site for the dislocations so that the dislocations may climb down from the surface. On the other hand, the tip of the defect at the substrate-film interface is clearly under a great amount of strain, so that it is possible that the dislocation first get injected at the tip, while a dislocation of inverse Burgers vector climbs up to the surface. Once the dislocations have climbed in the Si substrate over the length of the defect, they can easily glide to form a complete network of dislocations under the force exerted on them by the strain. The dislocation will be driven away from the interface and into the substrate because of the interaction energy between the newly formed dislocation and the defect. Indeed, if one assumes that the defect has a strain field and energy similar to an edge dislocation of equivalent Burgers vector, it is possible to estimate the equilibrium distance that the disloca-

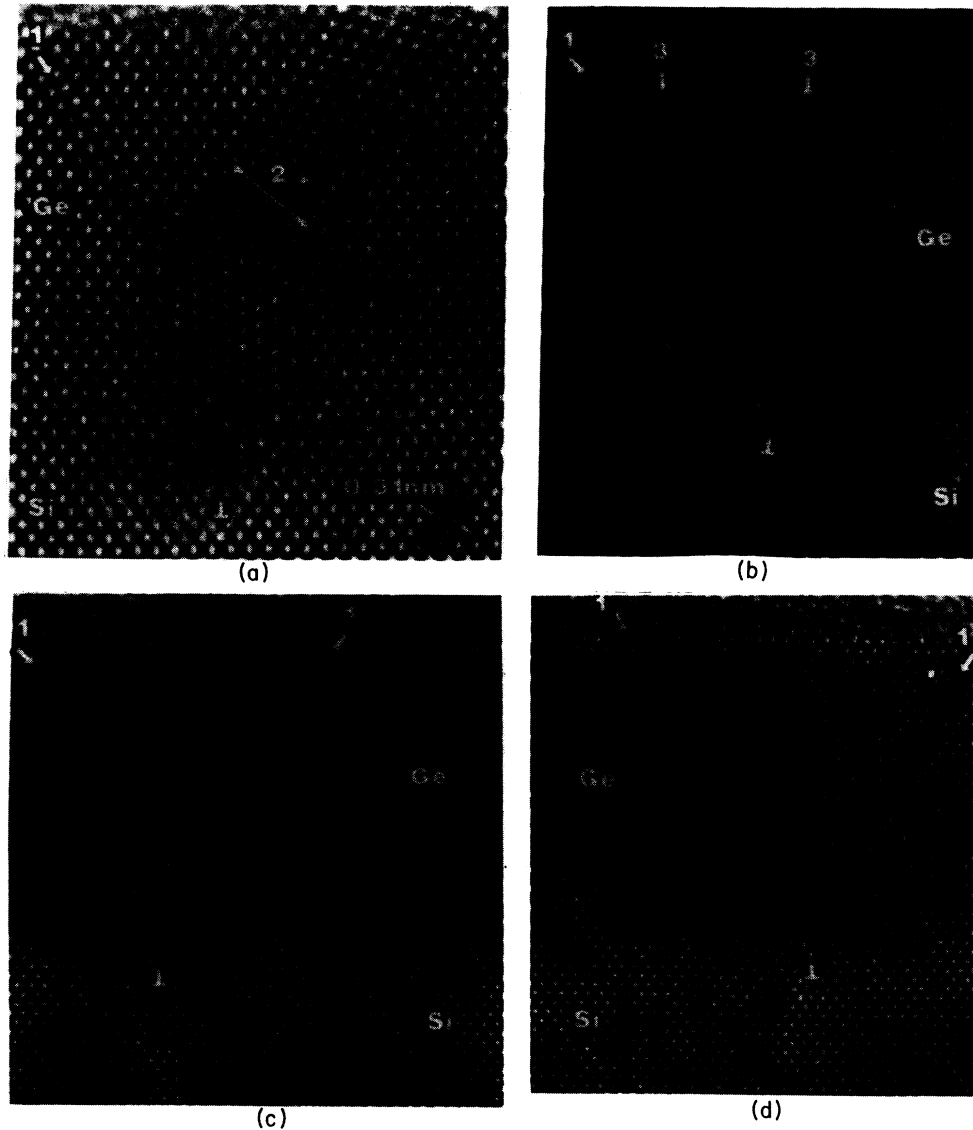


FIG. 9. Other defects in the 65-ML film. Arrows marked 1 show stacking faults. The arrow marked 2 shows a portion of the top layer that forms a twin with both the defect and the surrounding film. Arrows marked 3 show grain boundaries along the [001] direction generated by the defect.

tion has to climb into the Si substrate. We postulate that the Burgers vector of the defect is equivalent to the Burgers vector of a pure-edge dislocation which would relieve the same strain, equal to $0.13a$ per pair of tilted $\{111\}$ planes (the value 0.13 is the difference between the distance between two $\{111\}$ planes and its projection along the $[110]$ direction, or $1/\sqrt{2} - 1/\sqrt{3}$). The energy per unit length (W_{disl}/L) saved by moving two edge dislocations in the same material away from each other by a distance h is¹²

$$\frac{W_{\text{disl}}}{L} = \frac{-\mu}{2\pi(1-\nu)} b_1 b_2 \ln(h), \quad (1)$$

where μ and ν are Young's modulus and Poisson's ratio,

b_1 is the Burgers vector of an edge dislocation equivalent to the defect, b_2 is the Burgers vector of the pure edge dislocation moving in the Si, and L is the average length of the defect. The energy expanded to stress Si by inserting a network of dislocation into it is^{7,8}

$$\frac{W_{\text{stress}}}{D^2} = \frac{2\mu(1+\nu)}{(1-\nu)} \varepsilon^2 h, \quad (2)$$

where D is the average distance between dislocations and ε is the misfit generated by the network. By definition,

$$\varepsilon = \frac{b_2}{D}, \quad (3)$$

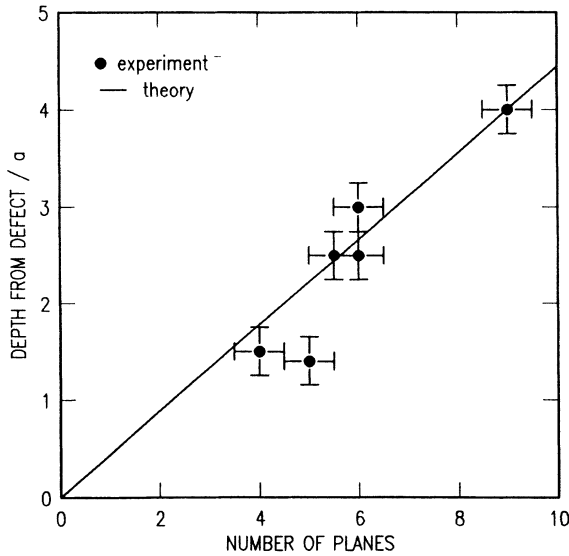


FIG. 10. Measured depth of the dislocation and theoretical curve obtained from Equation 6.

since b_2 is the Burgers vector of a pure edge dislocation, or $a/\sqrt{2}$, and the average distance between dislocations is measured to be 200 Å, ϵ is found to be equal to about 2%. Thus half of the 4% misfit between Si and Ge is relieved by dislocations and half by defects. We obtain the equilibrium depth h by minimizing the total energy of the system, thus writing

$$\frac{dW_{\text{disl}} + dW_{\text{stress}}}{dh} = 0. \quad (4)$$

This results in

$$h = \frac{b_1 b_2}{4\pi(1+\nu)} \frac{L}{\epsilon^2 D^2}, \quad (5)$$

substituting Eq. (3), in Eq. (5), we obtain,

$$h = \frac{L}{2a\sqrt{2}(1+\nu)} b_1. \quad (6)$$

L is determined experimentally to be about 200 Å. We see that the depth of the dislocation is directly proportional to the equivalent Burgers vector of the defect. Figure 10 shows measured values of h (Figs. 5 and 6 show how these points were obtained) as well as the theoretical values. The excellent agreement between theory and experiment has to be somewhat fortuitous since several assumptions were made to obtain the theoretical value. Nonetheless, the observed linear dependence directly results from the logarithmic dependence of W_{disl} with h . This logarithmic dependence is general for linear defects, and thus also applies for the tip of the V-shaped defects. Thus, although the slope may be different, the general form of Eq. (6) should be valid.

In order to remain in equilibrium, a dislocation has to adjust its depth locally as it meanders from one defect to another. The average depth of the dislocation network can be estimated by considering that, since defects take

care of half the misfit, on the average, each defect must have the Burgers vector of a full edge dislocation so that the average depth will be about 13 Å. Thus, the dislocation network changes the lattice parameter of (on average) the top 13 Å of Si and establishes a discontinuity in the lattice parameter, which explains the appearance of Moire fringes in Fig. 7. We can estimate the average distance necessary to fully relieve the misfit by considering that, on average, one defect and one associated dislocation have a Burgers vector of $a\sqrt{2}$ [see Fig. 6(b)]. This distance should be 190 Å, compared to 200 Å measured experimentally. In other words, at this point of the growth, the strain is either completely relieved, or only a small portion of it still needs to be relieved.

It was our hope that this mode of growth could be used to grow perfect, relaxed Ge layers, by burying the defects under an undefected, relaxed Ge layer. We have shown in Figs. 8 and 9 that this does not seem to happen often. The main reason for this is probably that, in order to cover the defect with Ge having the same orientation as the Si substrate, an incoherent boundary has to be created at the top of the defect. This boundary would have a considerably higher energy than a simple twin, which can be achieved as in the configuration shown in Fig. 9(a). The stacking faults observed at the top of most of the defects probably tend toward the same goal. They may also play another role: stacking faults in this configuration are also partial (or threading) dislocations, and are the last mechanism to completely relieve the strain in this system.

V. CONCLUSIONS

Up to now, it was generally believed that the critical thickness for establishing a dislocation network is determined by the energy needed to *move* a (preexisting) dislocation. This assumes that there must be a low-energy *source* of dislocations. Looping from the surface was proposed as a mode of dislocation nucleation for a perfect, layer-by-layer grown film. We have shown that, at least for the case of Ge/Si(001), looping does not occur. During normal growth (islanding), dislocations do indeed form, but they must form at the edges of islands generated at the early stages of growth, or at other defects at the interface. On the other hand, when layer-by-layer growth is achieved, this system goes through three different mechanisms to relieve the misfit. First, rather complicated V-shaped defects are formed homogeneously and catastrophically. These defects have too high an energy to keep growing and completely relieve the strain and, more importantly, they can act as injection sites for dislocations. These dislocations then glide to previously undefected areas in the Si substrate to form a continuous network. Further growth generates numerous stacking faults and twins around the previously formed defects. These likely play a role in minimizing boundary energies between the defect and its surrounding. They may also relieve any remaining strain left after the two previous mechanisms have operated.

The literature abounds with confusing discrepancies

between “theoretical” and experimental critical thicknesses. We feel that the assumptions of Matthews and Blakeslee’s theory, while justified in some (maybe many) cases, are not generally fulfilled. Hence, an indiscriminate comparison of critical thicknesses derived from this theory with experimental results is bound to re-

sult in apparent disagreement. The central issue, sidestepped in many studies, is where and how the dislocations (and/or defects) are generated in the first place. This may be different from system to system, from growth condition to growth condition, and even from sample to sample.

¹M. Copel, M. C. Reuter, and R. M. Tromp, *Phys. Rev. Lett.* **62**, 632 (1989).

²M. Copel, M. Horn Von Hoegen, and R. M. Tromp, preceding paper, *Phys. Rev B* **42**, 11 682 (1990).

³F. K. LeGoues, M. Copel, and R. M. Tromp, *Phys. Rev. Lett.* **63**, 1826 (1989).

⁴The parameters used for the multislice calculations were as follows: aperture size, 10 nm; thickness of sample, 9.2 nm; spherical aberration, 1 mm; focus spread, 5 nm; beam semi-convergence, 0.5 mrad; defocus, 50 nm (Sherzer). For more detail on the simulations, see P. A. Stadelmann, *Ultramicroscopy* **21**, 131 (1987).

⁵J. H. van der Merwe, *J. Appl. Phys.* **34**, 117 (1963).

⁶J. T. Wetzel, A. A. Levi, and D. A. Smith, *Trans. Jpn. Inst. Met.* **27**, 1061 (1986).

⁷R. E. Thomson and D. J. Chadi, *Phys. Rev. B* **29**, 889 (1984).

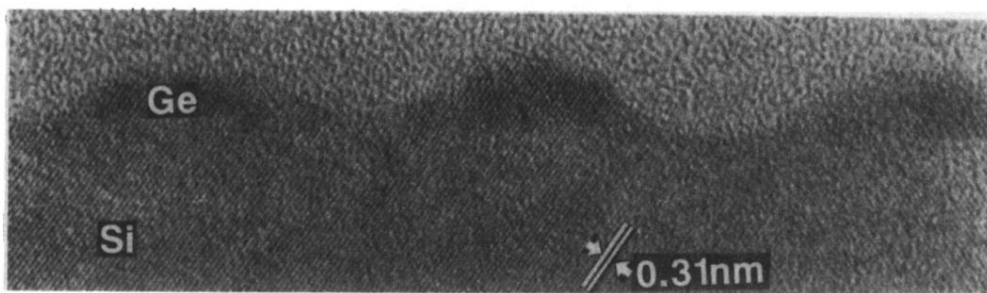
⁸J. W. Matthews and A. E. Blakeslee, *J. Cryst. Growth* **29**, 273 (1975).

⁹J. W. Matthews and A. E. Blakeslee, *J. Cryst. Growth* **27**, 118 (1974).

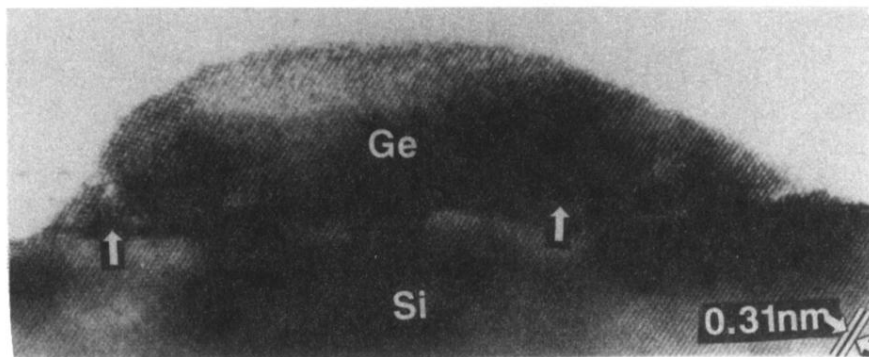
¹⁰D. J. Eaglesham and M. Cerullo, *Phys. Rev. Lett.* **64**, 1943 (1990).

¹¹M. Chilsholm and P. D. Kirchner (private communication).

¹²J. P. Hirth and J. Lothe, in *Theory of Dislocations* (McGraw-Hill, New York, 1968).



(a)



(b)

FIG. 1. Cross-sectional views of samples grown without surfactant. (a) 8 monolayers. Note that the islands are still pseudomorphic. (b) 15 monolayers. Arrows indicate the presence of dislocations at the interface between the island and the substrate.

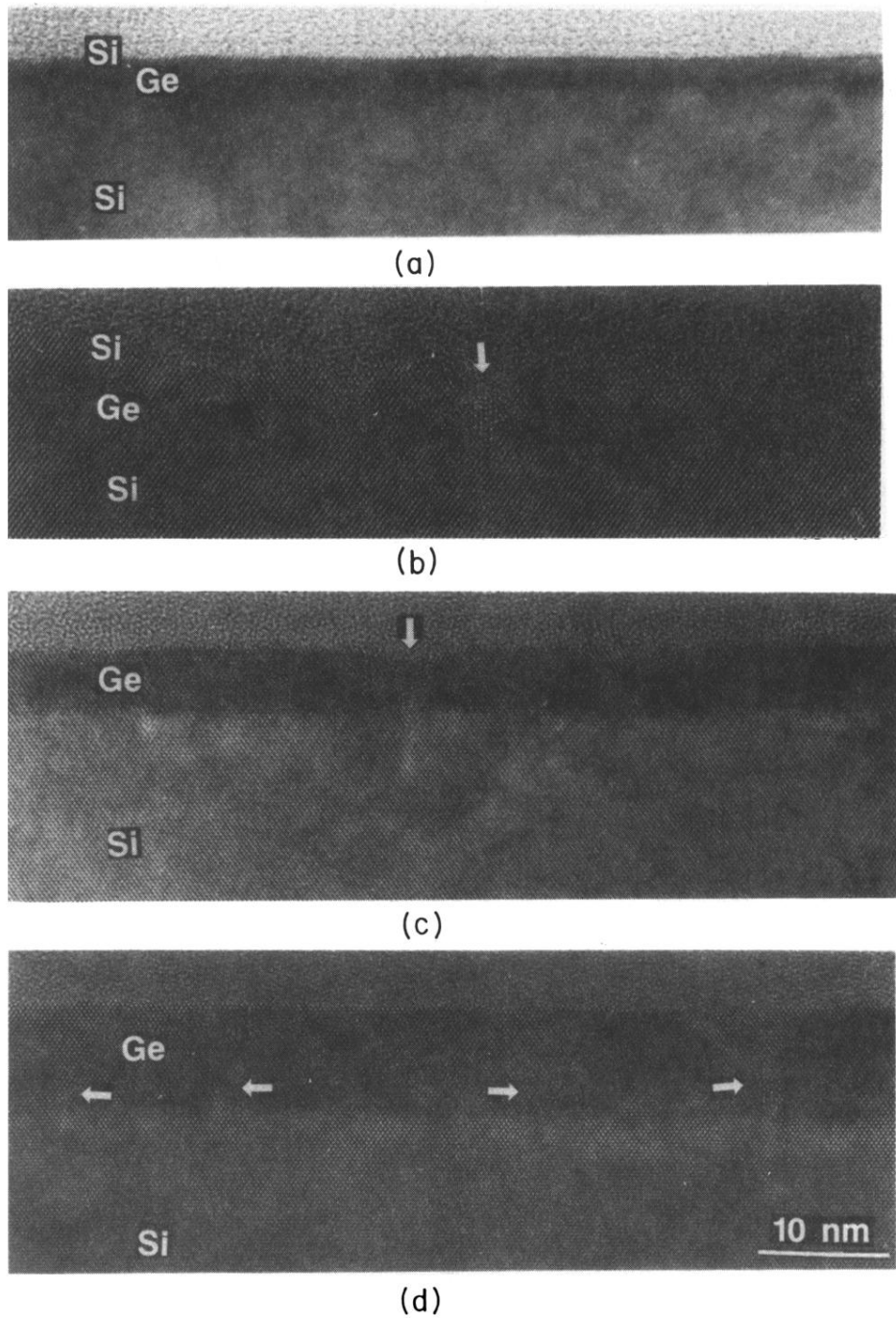


FIG. 2. Cross-sectional views of the samples grown with an arsenic surfactant. (a) 8 monolayers; (b) 12 monolayers; (c) 50 monolayers; (d) 65 monolayers.

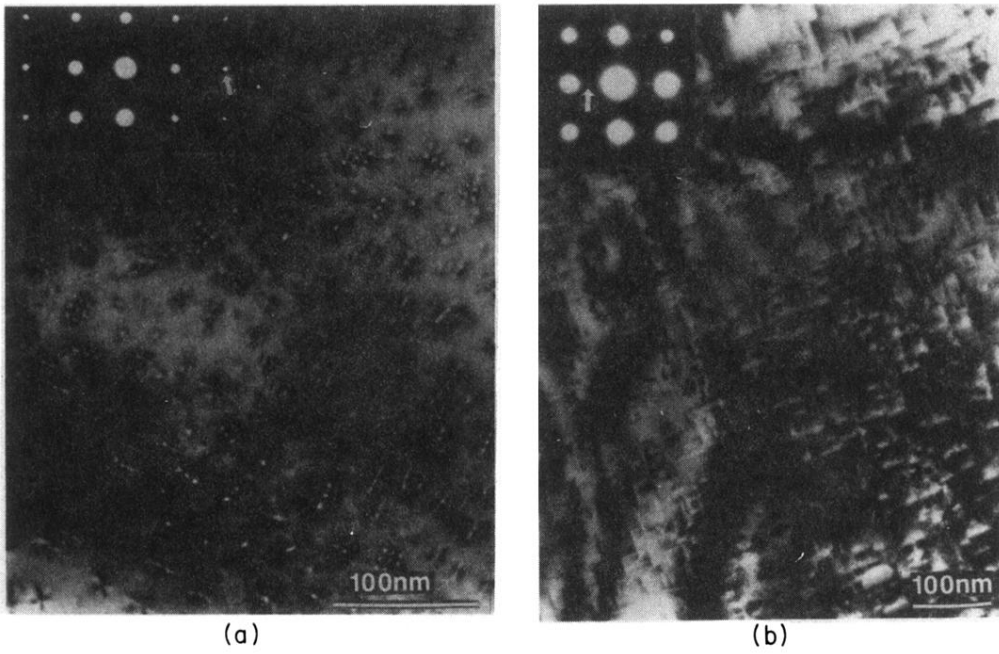


FIG. 3. Planar view of 12 monolayers grown on (a) bare Si and (b) arsenic passivated Si. The arrow on the diffraction pattern on (a) indicates the splitting of the spots showing that Ge has the lattice parameter of bulk Ge. The arrows on (b) show the extra spots associated with the V-shaped defects.

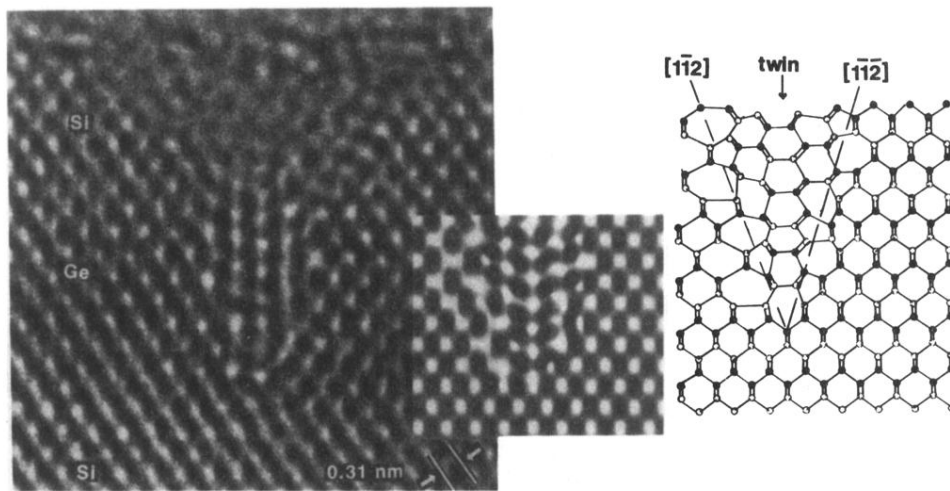


FIG. 4. Cross-sectional view of one defect in the 12-ML film, atomic model, and corresponding image simulation (the parameters for the simulations are described in Ref. 11).

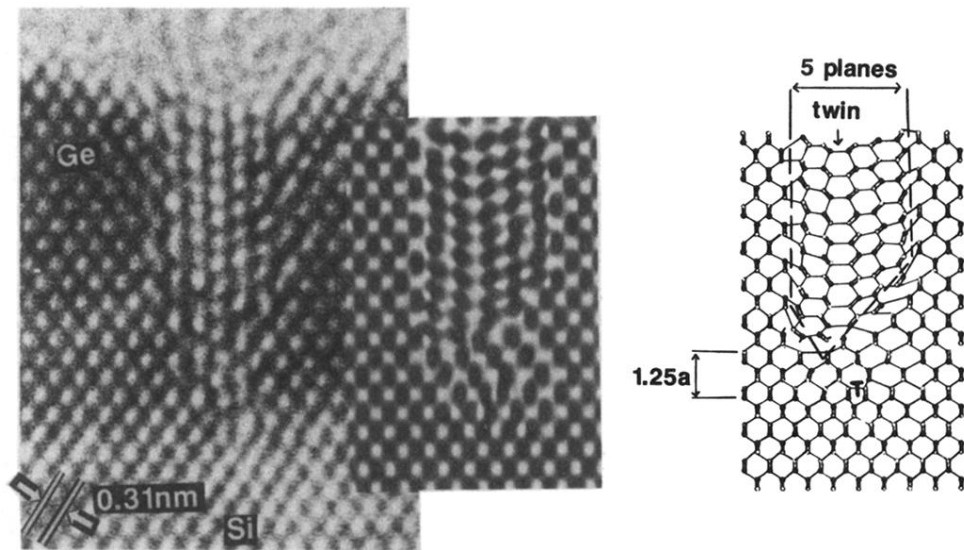


FIG. 5. Cross-sectional view, atomic model, and simulation of one defect in the 50-ML film.

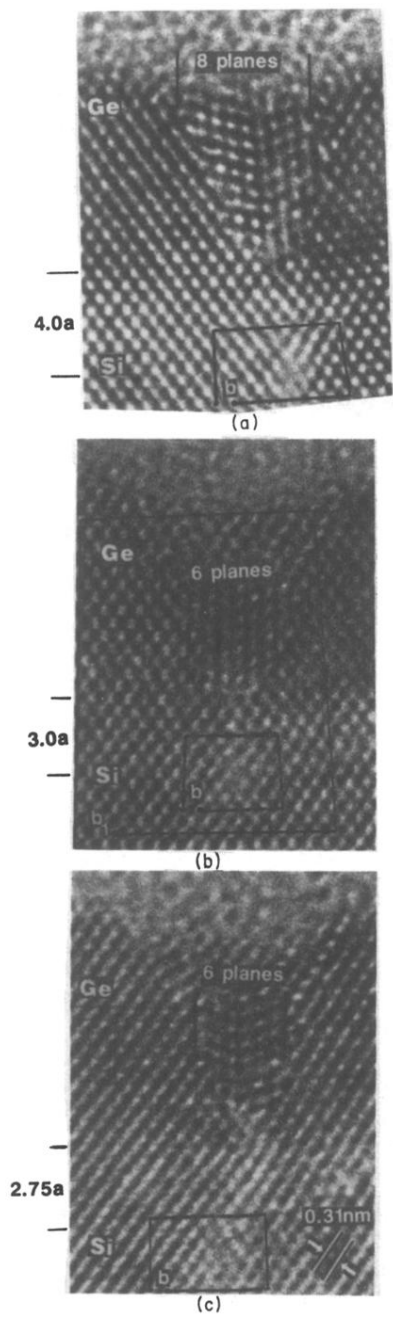


FIG. 6. Other defects found in the 50-ML film. Burgers circuit have been drawn, entirely contained in the Si substrate, that locate the edge dislocations. In (b), a Burgers circuit has also been drawn around the defect to demonstrate that it is equivalent to a dislocation.

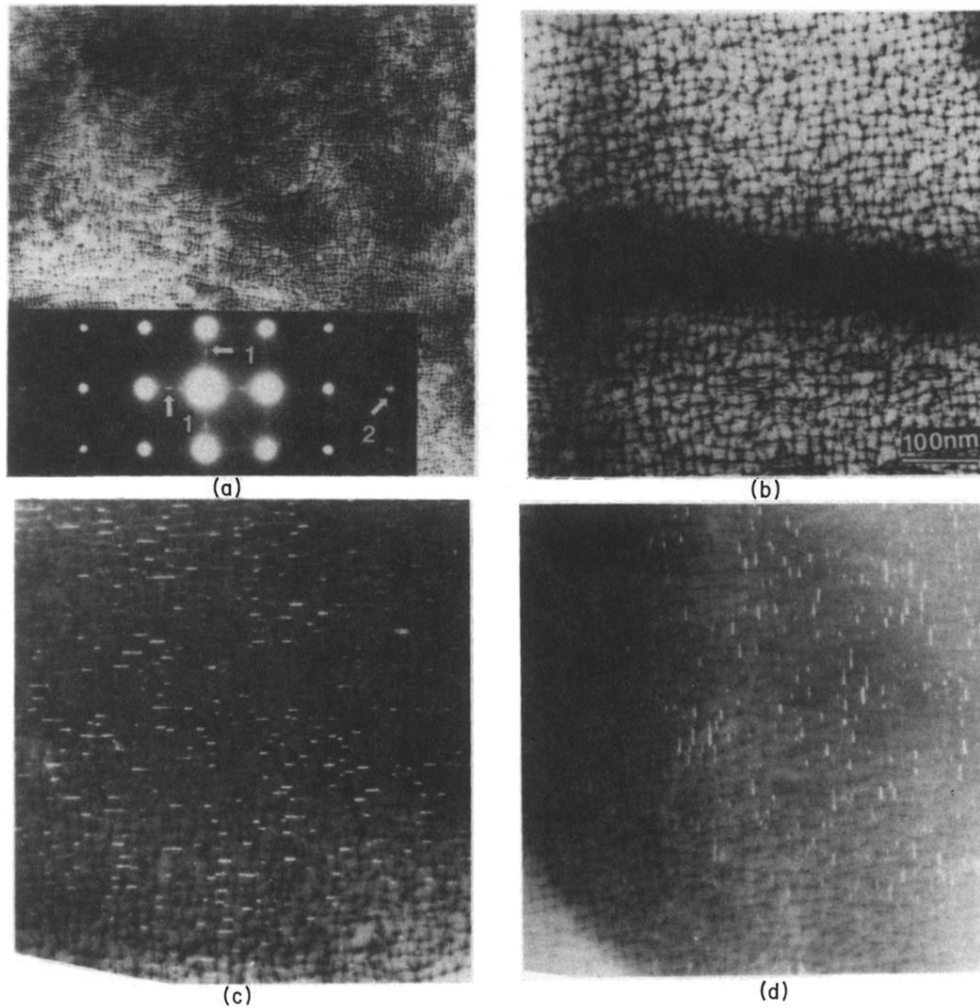


FIG. 7. Planar view of the 50-ML sample. (a) The zone axis is exactly [001], or perpendicular to the substrate. Arrows in the diffraction pattern indicate the extra reflections due to the defects. (b) Same area. The sample has been tilted off the exact zone axis by a few degrees in order to lower the contrast of the Moire fringes and image the dislocation network. (c) and (d) Dark field micrographs obtained using the reflections marked by arrows in (a).

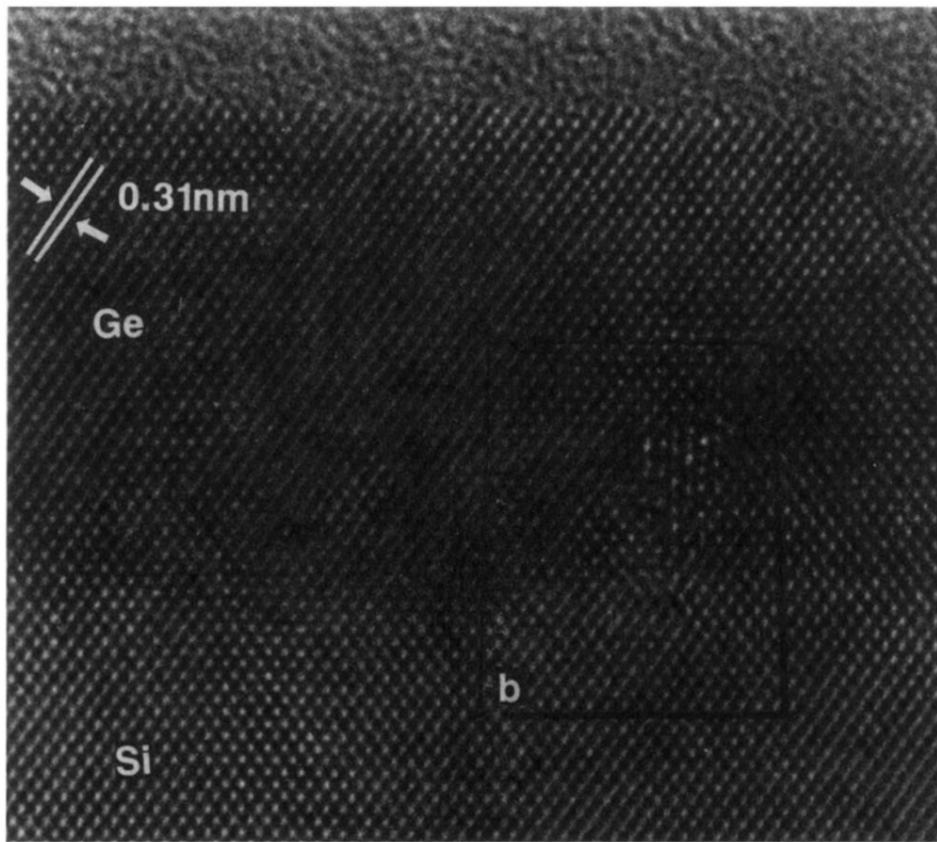


FIG. 8. One defect in the 65-ML film that has been completely covered by undefected Ge. A Burgers circuit has been drawn around the defect, and its associated dislocation, which show that, together, they are equivalent to two pure edge dislocations.

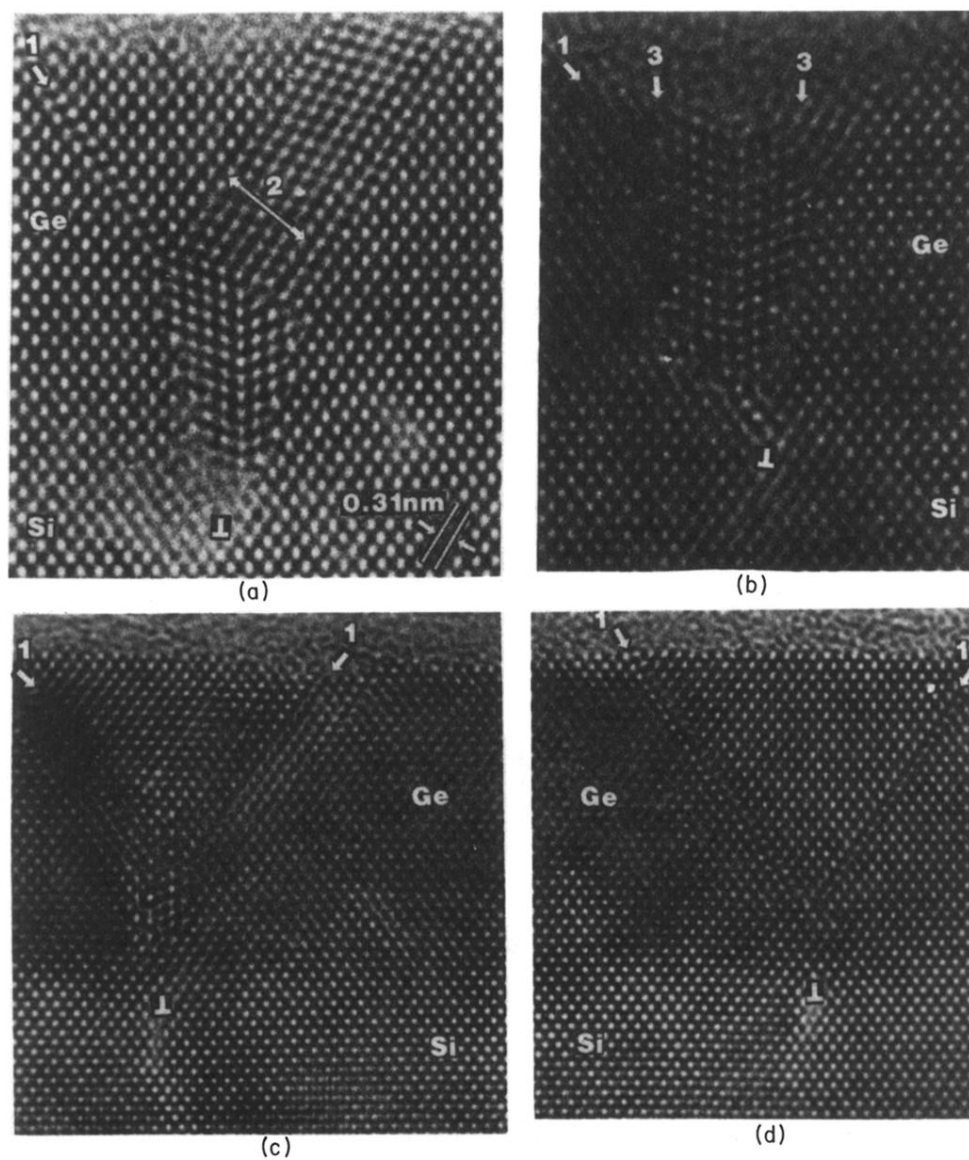


FIG. 9. Other defects in the 65-ML film. Arrows marked 1 show stacking faults. The arrow marked 2 shows a portion of the top layer that forms a twin with both the defect and the surrounding film. Arrows marked 3 show grain boundaries along the [001] direction generated by the defect.